CREEP DAMAGE MECHANICS AND MICROMECHANISMS

M. F. Ashby* and B. F. Dyson**

**Engineering Department, University of Cambridge, Trumpington Street, Cambridge, England*
***National Physics Laboratory, Division of Materials Applications, Queen's Road, Teddington TW11 OLW, England*

ABSTRACT

Creep fracture is the end result of the accumulation of damage during creep. In this paper, micromechanisms of damage are classified, and a methodology of analysis is developed. For each mechanism, a damage-evolution law and a creep-law is derived. The result is a pair of differential equations, with the same form as that of the continuum treatment of Kachanov and Rabotnov. The equations can be integrated to give the shape of the creep curve, the time and strain to fracture, residual life, and so forth. Each mechanism exhibits a characteristic shape of creep curve, with an associated Monkman-Grant constant and creep ductility; these give guidance in selecting and using the appropriate equations. Progress is made in unifying the continuum and micromechanistic approaches to creep fracture, and a method is presented for identifying the dominant damage mechanism (or class of mechanism) from the shape of the tensile creep curve.

An overview of the contents of this paper can be obtained by reading Sections 1, 2, 3 and 5.

KEY WORDS

Creep damage; tertiary creep; creep fracture; mechanisms of creep fracture; damage mechanics.

SYMBOLS AND UNITS

σ	Tensile stress (MPa)
$\dot{\epsilon}$	Tensile strain-rate (s^{-1})
ϵ	Tensile strain
T	Temperature (K)

t	Time (s)
w, w_1, w_2 ...	Damage
w_c	Terminal damage
$\dot{\epsilon}_m$	Initial, or minimum creep rate (s^{-1})
t_f	Time to failure (s)
ϵ_f	Strain to failure
ϵ^*	Critical strain to fracture oxide
C_m	Monkman-Grant constant, $\epsilon_m \; t_f$
λ	Creep-damage tolerance, $\dot{\epsilon}_f/\dot{\epsilon}_m \; t_f$
E	Young's modulus (GPa)
G	Shear modulus (GPa)
σ_o, $\dot{\epsilon}_o$, n	Constants in the creep law, eqn. (3.3) (MPa, s^{-1}, -)
$\dot{w}_o$, m	Constants in the damage law, eqn. (3.3) (s^{-1}, -)
σ_y	Yield strength (MPa)
h	Work-hardening exponent
σ_p	Threshold stress due to particles (MPa)
σ_p^o	Initial threshold stress due to particles (MPa)
σ_i	Internal stress (MPa)
H	Hardening rate (MPa)
R	Recovery rate (s^{-1})
r_h	Void radius (in boundary plane) (m)
2ℓ	Void spacing (m)
R	Radius of cylindrical sample (m)
r	Particle radius (m)
r_o	Initial particle radius (m)
$2\ell_p$	Particle spacing (m)
$2\ell_o$	Initial particle spacing (m)
L	Slip distance (m)
f	Volume fraction of particles
x	Depth of internal oxidation (m)
c	Crack length (m)
d	Grain diameter (m)
ϕ_o, ψ_o	Dimensionless material properties
γ	Surface energy of void (J/m^2)
ρ	Dislocation density (m^{-2})
α	A constant (roughly $\frac{1}{3}$)
K, K', K_p	A kinetic constant (m^2/s)
k	Boltzmanns constant (1.38×10^{-23} J/K)

INTRODUCTION

Creep-damage is a term coined by engineers to describe the material degradation which gives rise to the acceleration of creep rate known as tertiary creep. It is the central concept in the mechanics of creep fracture developed by Rabotnov (1969), Hult (1974) Leckie (1977) and his collaborators from a seminal idea of Kachanov (1958). The material is treated as a continuum and, since the detailed processes of degradation are not examined, assumptions or postulates are made to describe the rate of damage evolution. The usual assumptions (described in Section 3) have a certain generality which allows the resulting equations to be fitted to experimental data with a degree of success; but they are not based on microstructural observations or physical reasoning.

The material scientist studying creep is disturbed by this vague description of damage. His unease is reinforced by recent attempts to model the growth of holes or cracks during creep which can lead to equations which do not appear to resemble those of the continuum treatment. He is further concerned by the obvious experimental fact that there are several mechanisms of creep-damage, while the continuum equations appear to describe only one.

If progress is to be made in developing a Mechanics of Creep-Damage, these two approaches must be reconciled and the strengths and weaknesses of each recognized. The present paper attempts to do this by developing a general methodology for the description of tertiary creep. Models for each mechanism are presented as illustrations, while acknowledging that, in many instances, they are unrealistically simple.

CATEGORIES OF CREEP DAMAGE

We distinguish four broad categories of creep-damage while recognising that each may contain more than one mechanism. They are described in Sections 2.1 to 2.4 and illustrated in Fig. 1. Any one mechanism operating alone can cause final fracture or rupture. More usually, fracture is the result of the operation of two or more mechanisms, sometimes operating sequentially, sometimes simultaneously.

Damage by Loss of External Section

Deformation at constant volume causes a shape change. During creep under a constant tensile load, the section decreases, stress slowly increases and the creep rate accelerates (Fig. 1a and 1b). In the absence of other damage mechanisms, failure occurs when the material necks to a point. Usually, other damage mechanisms (discussed below) intervene and lead to failure at a finite reduction in the area (that is fracture intervenes); but at very high temperatures (above 0.8 T_M, where T_M is the melting point) pure metals and solid solution alloys often rupture by this mechanism alone, as shown in Fig. 2. In compression, of course, the section increases and the creep rate falls; then the damage must be regarded as negative.

Damage by Loss of Internal Section

(a) Formation of holes at grain boundaries. The mechanism most widely studied experimentally and modelled theoretically is hole formation, or cavitation, either within the grains (Fig. 1c) or at grain boundaries (Fig. 1d). Most commonly, the holes appear on boundaries which lie roughly perpendicular to the maximum principal tensile stress direction (Fig. 1(d)).

Their presence reduces the section and so accelerates the creep and this, in turn, increases the rate at which the damage grows. At low stresses the damage is void-like; at high, the voids may link to give grain-boundary cracks (Fig. 1d). Many pure metals and industrial alloys can fracture by this mechanism alone (including the important nickel-base superalloys and the ferritic and austenitic steels), though it is more usual for other mechanisms to contribute also. The holes take on a variety of shapes depending on their spacing and on the temperature and strain rate. The characteristic appearances of low and high ductility fracture are shown in the optical micrographs in Figs. 3 and 4. The latter shows how damage mechanisms interact: cavitation has terminated life in a material in which tertiary creep was due to degradation of the substructure (see below) followed by necking.

(b) Growth of single dominant cracks. An industrial component often has a spatially-inhomogeneous stress distribution which may result in the formation of a discrete crack (often caused by localised creep cavitation), which then generates an even smaller zone of damage around its tip (Fig. 1e). Growth of these discrete cracks (Fig. 5) is thought to be important in thick-sectioned components (found in electricity-generating and petrochemical plants) where the system stresses are low and the design-lives are long.

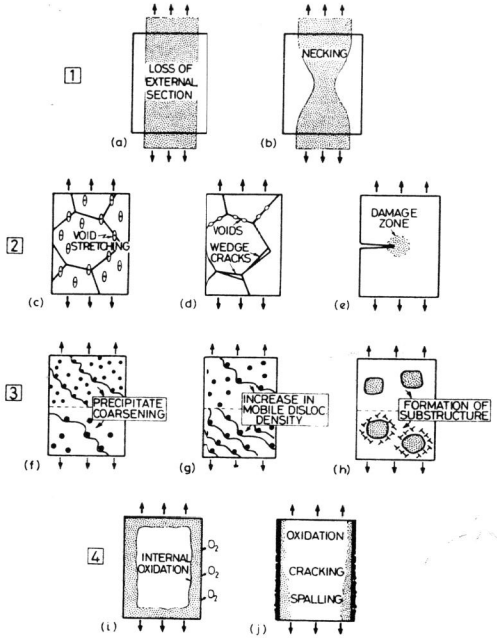

Fig. 1. The four categories of creep damage: (i) loss of external section; (ii) loss of internal section by voiding, or cracking; (iii) damage by degradation of the microstructure; (iv) damage caused by interaction with the environment.

Damage by Degradation of the Microstructure

(a) Thermal-coarsening of particles. Many alloys in service under load at high temperatures are deliberately strengthened by second-phase particles: γ' in superalloys, intermetallics in aluminium alloys, carbides in ferritic and austenitic steels. During creep, these coarsen, or are replaced gradually by more stable particles; both forms of ageing can accelerate creep (Fig. 1f). Figure 6a shows how ageing accelerates the creep rate of the superalloy

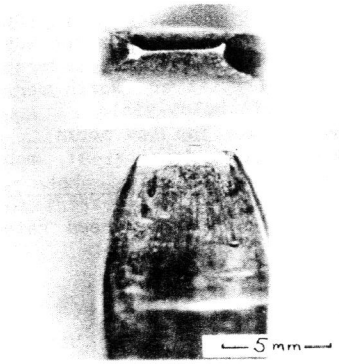

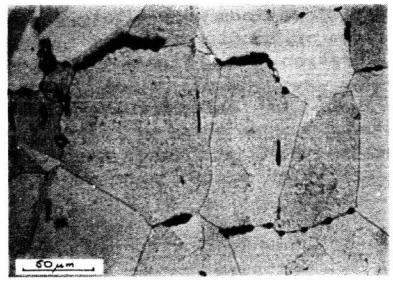

Fig. 2. Damage by loss of external section; necking to a point (pure aluminium, 375 °C, 2.5 MPa, t_f = 353 h; courtesy T.B. Gibbons and R.K. Varma).

Fig. 3. Damage by loss of internal section: cavitation in Nimonic 105 nickel-base superalloy with lead as a trace impurity (815 °C, 232 MPa, ε_f = 9 %, R.A. = 9.6 %, t_f = 1200 h; stress axis vertical; courtesy G.B. Thomas).

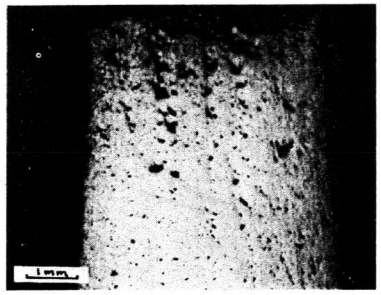

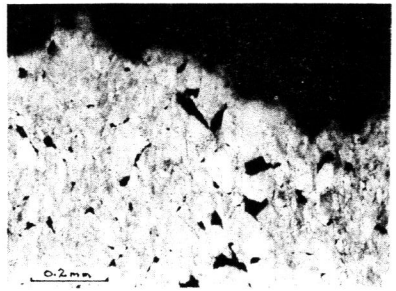

Fig. 4. Damage in Nimonic 105 of normal purity. The dominant damage is sub-structural, but failure is caused by cavitation plus necking (850 °C, 200 MPa, ε_f = 26 %. R.A. = 51 %, t_f = 399 h).

IN738LC when stresses are high (approaching the athermal yield stress). At low stresses, on the other hand, prior ageing has little or no change in creep rate, as shown in Fig. 6. And even in the high stress tests, the reduction in creep resistance due to aging was not sufficient to account for most of the acceleration in creep rate observed during tertiary creep. Some other mechanism is contributing simultaneously to damage accumulation. This lead us to consider a second kind of microstructural change, associated with the dislocation substructure.

(b) Substructure-induced acceleration of creep. Although particle-coarsening can account for some observations of tertiary creep without loss of section, it is unable to explain data for a large family of nickel-based superalloys (Dyson and McLean, 1983). Here an acceleration of creep is associated with the way in which dislocations accumulate during creep. This is the least-well understood mechanism of tertiary creep. At present, two possibilities are worth serious consideration. The first is that, at low stresses, well below yield ($\sigma \approx 0.1\ \sigma_y$), dislocation motion is climb-controlled. The low mobility can then lead to deformation which is limited by the density of mobile dislocations: as this increases, the creep rate accelerates (Fig. 1g). The second is that, at higher stresses ($\sigma \approx 0.5\ \sigma_y$), a cellular network forms (Fig. 7) which allows more rapid recovery, and an accelerating creep rate (Fig. 1h).

Damage by Gaseous- Environmental Attack

a) Damage by internal oxidation. Exposure to aggressive gasses before or during creep often accelerates creep and reduces the life. If a component is

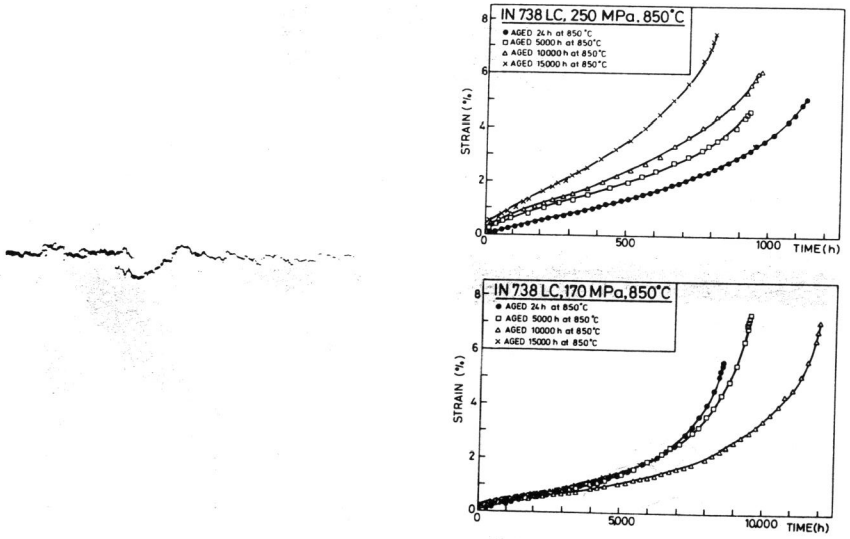

Fig. 5. A creep crack in a creep-resistant steel (½ % Cr Mo V steel tested at 565 °C; courtesy G.A. Webster).

Fig. 6. Creep acceleration caused by ageing (IN 738 LC, 850 °C, 250 MPa). Data from Tipler and Peck (1981).

heated in an oxidising atmosphere, for example, oxygen penetrates the metal (unless, of course, it forms a protective surface oxide which remains intact during creep). The inward-diffusing oxygen reacts with impurities to give a zone of internal oxidation (Fig. 1(i) and Fig. 8). In this zone, gas bubbles (CO_2, H_2O) may form on grain boundaries; or precipitated solid oxide may act as nuclei for voids. Both the bubbles and the voids degrade the strength within the zone.

(b) Damage by failure of external oxide. Creep can disrupt an otherwise-protective surface film, by straining it until it fractures (Fig. 1(j) and Fig. 9). If it does, environmental attack restarts at the cracks, or spalls, which may also act as sources for internal oxidation.

Each of these mechanisms is examined in more detail in Section 4. Some are well studied and understood; others have received only scant attention. For each mechanism we seek to derive an equation describing the rate at which damage accumulates, and an associated equation for the rate at which the material creeps. This pair of equations completely describes creep in the material if that mechanism operates alone. The formalism is that of continuum creep-damage mechanics, which we now review.

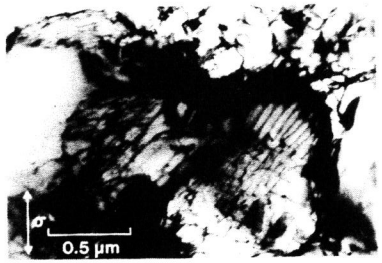

Fig. 7. The dislocation network formed in a nickel-based superalloy by creep (IN 738, 850 °C, 270 MPa, ε_f = 6 %, t_f = 506 h.; courtesy P.J. Henderson, 1984).

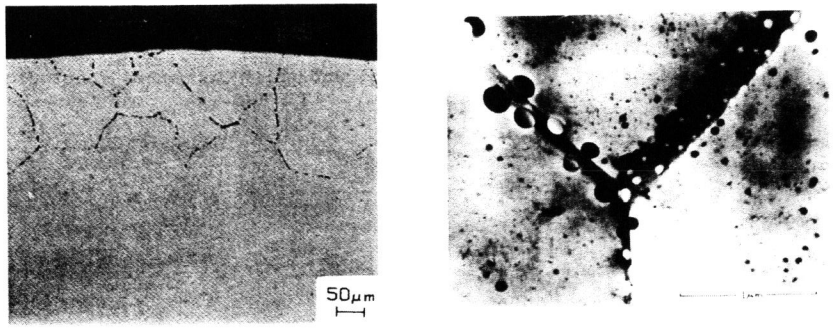

Fig. 8. Damage by internal oxidation (a) subsurface damage in nickel caused by internal oxidation (courtesy R.H. Bricknell and D.A. Woodford, 1982, and Acta Metallurgica); (b) internal oxide particles at high magnification.

CREEP DAMAGE MECHANICS

The Continuum Formalism

Creep-damage mechanics (Kachanov, 1958; Hult, 1974; Rabotnov, 1969; Leckie and Hayhurst, 1977) has developed as a continuum-mechanical approach to the analysis of creep fracture. In its simplest form, damage is measured by the scalar parameter w which varies from zero (when no damage is present) to one (at failure). Both damage w and strain ε are assumed to grow with time in a way which depends on stress σ, and on temperature T and on the current extent of the damage w so that, for simple tension:

$$\frac{dw}{dt} = g\,(\sigma,\ T,\ w)$$
$$\frac{d\varepsilon}{dt} = f\,(\sigma,\ T,\ w) \qquad (3.1)$$

The creep life, the strain to failure, and the shape of the creep curve are obtained by integrating the equations between the appropriate limits. They can be extended to include primary creep (Hult, 1974), multiaxial stresses (Leckie and Hayhurst, 1977) when w may have to be treated as a tensor.

To proceed further, explicit functions are assumed for f and g. It is common practice to represent the creep of crystalline solids by Norton's law. Then the minimum creep rate $\dot{\varepsilon}$ is related to the tensile stress σ by

$$\frac{d\varepsilon}{dt} = \dot{\varepsilon}_o \left(\frac{\sigma}{\sigma_o}\right)^n \qquad (3.2)$$

where $\dot{\varepsilon}_o$ is a temperature-dependent creep parameter and n is a constant exponent. This suggests (Rabotnov, 1969; Leckie and Hayhurst, 1977) the following forms for the damage rate:

$$\frac{dw}{dt} = \dot{w}_o \left(\frac{\sigma}{\sigma_o\,(1 - w)}\right)^m \qquad (3.3a)$$

$$\frac{d\varepsilon}{dt} = \dot{\varepsilon}_o \left(\frac{\sigma}{\sigma_o\,(1 - w)}\right)^n \qquad (3.3b)$$

Here $\dot{w}_o$ is a temperature-dependent rate constant (like $\dot{\varepsilon}_o$) and m is a constant exponent (like n). Note that the equations lead to a damage rate dw/dt which is finite even when w is zero, and which increases monotonically with w. Procedures for determining n, m, $\dot{\varepsilon}_o$ and. $\dot{w}_o$ are described by Leckie and Hayhurst (1977).

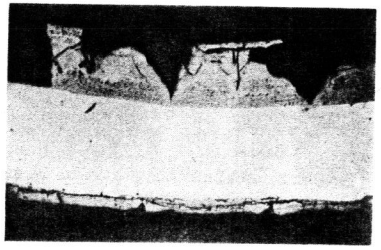

Fig. 9. Damage by external oxidation (courtesy Bara and Peters, 1970 and Gordon and Breach).

The great attraction of this formalism is in its generality. Equations (3.3) are easily integrated as a coupled set to give the shape of the creep curve, the time to fracture t_f and the strain to fracture ε_f (an example is shown in Fig. 10). The effect of stresses which vary with time, or non-steady temperatures, can be computed (although true primary creep and transients associated with stress or temperature change are neglected in the simple eqns. (3.3)).

We now introduce three important properties of the material: the Monkman Grant constant C_m, the strain to failure ε_f, and the creep damage tolerance, λ. The constant C_m (Monkman and Grant, 1956) is the minimum strain rate $\dot{\varepsilon}_m$ times the time to fracture t_f. Integrating eqn. (3.3a) from $w = 0$ to $w = 1$, at constant stress, gives:

$$C_m = \dot{\varepsilon}_m\, t_f = \left(\frac{1}{1 + m}\right) \frac{\dot{\varepsilon}_o}{\dot{w}_o} \left(\frac{\sigma}{\sigma_o}\right)^{n-m} \qquad (3.4)$$

Integrating eqn. (3.3b) gives the strain to failure ε_f:

$$\varepsilon_f = \left(\frac{1}{m + 1 - m}\right) \frac{\dot{\varepsilon}_o}{\dot{w}_o} \left(\frac{\sigma}{\sigma_o}\right)^{n-m} \qquad (3.5)$$

Finally, the creep damage tolerance, λ, (Leckie and Hayhurst, 1977) is defined by:

$$\lambda = \frac{\varepsilon_f}{\dot{\varepsilon}_m\, t_f} = \left(\frac{m + 1}{m + 1 - n}\right) \qquad (3.6)$$

At fracture, the strain is $\lambda\, \dot{\varepsilon}_m\, t_f$. The quantity λ measures the tolerance of the material to strain concentrations. Its value for engineering alloys ranges from 1 to about 20. A low λ is undesirable because cracks will initiate at strain concentrations (like holes or changes of section) where the local strain is larger than the general strain. A large λ means that the material can tolerate strain concentrations without local cracking.

We now seek to analyse the micromechanisms, describing each by a pair of coupled equations like eqns. (3.3), and evaluating for each the quantities C_m, ε_f and λ.

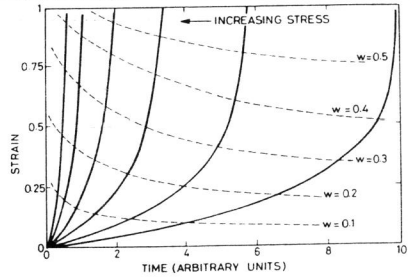

Fig. 10. Creep curves resulting from the integration of eqns. (3.3). The broken lines show contours of constant damage ($n = 4$, $m = 5$).

THE MODELLING OF CREEP DAMAGE

We have seen (Section 2) that tertiary creep, leading ultimately to failure, can be caused by many different mechanisms. Here we analyse each, expressing the damage-rate and the strain-rate in the form of eqns. (3.3). This reveals both the common ground and the fundamental differences between the continuum and the microscopic treatments of creep-damage, and it suggests ways in which the continuum method might be modified to include information about mechanisms.

The mechanisms can occur simultaneously. It is simplest to analyse them separately, when one finds, often, that regimes of stress and temperature exist over which one mechanism is overwhelmingly dominant, so that damage accumulation is adequately described by taking it alone. But this is not always true: the coupling of mechanisms can sometimes be of major importance. Commonly, a single mechanism (like the diffusional void growth of Fig. 1d) is dominant for most of the life, but final fracture is caused by the intervention of a second mechanism (ductile tearing, involving extension of voids by power-law creep, as in Fig. 1c, for instance). Then the time to fracture, but not the strain to fracture, can be calculated with acceptable accuracy by assuming the first mechanism acts alone.

Damage by Loss of External Section

(a) Loss of external section without necking. When a bar creeps under a constant tensile force F, its length will increase at an accelerating rate because of the decrease in cross-section, A (Hoff, 1953, and Fig. 11). This loss of section is a sort of damage. Define the damage by:

$$w_i = 1 - A/A_i \qquad (4.1)$$

where A_i is the initial section. The initial stress is:

$$\sigma = F/A_i$$

where F is the tensile force. Then it follows that:

$$\frac{dw_i}{dt} = \dot{\varepsilon}_m \left(\frac{1}{1 - w_i}\right)^{n-1} \qquad (4.2a)$$

$$\frac{d\varepsilon}{dt} = \dot{\varepsilon}_m \left(\frac{1}{1 - w_i}\right)^{n} \qquad (4.2b)$$

These have almost - but not exactly - the form of eqns. (3.3). Integrating eqns. (4.2) gives the time to failure, t_f, in terms of the strain to failure, ε_f.

$$C_m = \dot{\varepsilon}_m t_f \frac{1}{n}\left(1 - \exp\left(-n\,\varepsilon_f\right)\right) \qquad (4.3)$$

where the minimum creep rate, $\dot{\varepsilon}_m$, is given by:

$$\dot{\varepsilon}_m = \dot{\varepsilon}_o \left(\frac{\sigma}{\sigma_o}\right)^n \qquad (4.4)$$

If $n\,\varepsilon_f \gg 1$ then $C_m \approx 1/n$ and the creep-damage tolerance λ is given by:

$$\lambda = \frac{\varepsilon_f}{\dot{\varepsilon}_m t_f} \approx \infty \qquad (4.5)$$

The shape of the creep curve is obtained by integrating eqns. (4.2) as a coupled set. In reality ε_f and λ are infinite only in the special case of Newtonian viscous creep, as in the drawing of glass fibres. In all other cases, another mechanism intervenes. The most obvious is necking, which we consider next.

(b) Loss of external section with necking. In tension, steady-state creep is intrinsically unstable. If one part of the sample has a slightly smaller section than the rest, then the stress there is higher, the creep rate larger and the difference in section is amplified (Fig. 12). This reasoning has lead to statements that there can be no steady creep in tension; but the reasoning is incomplete. The proper question is not: when will a perturbation in the section be amplified? It is: when will the rate of amplification be large enough to influence the creep rate, and the life of the sample, significantly?

A rigorous answer is still not available. But approximate analyses (Hart, 1967; Burke and Nix, 1975) give a fairly complete picture. First, the question of stability. A criterion for stable deformation in tension (Hart, 1967) is obtained by considering the stability of a perturbation δA in the cross-section of a sample of section A, made from a material with creep exponent n and strain-hardening constant h (so that work hardening is described by $\sigma_y = \sigma_{oy} \exp h\varepsilon$). It is readily shown (Hart, 1967) that the perturbation does not grow, and deformation is stable, if:

$$h + 1/n \geq 1 \qquad (4.6)$$

This result is consistent with two well-known limits. For a rate-independent solid ($n = \infty$), the criterion reduces to that of Considere (1885). For a Newtonian-viscous material ($n = 1$, $m = 0$) it predicts stable deformation at all strains. But it also indicates that a power-law creeping material ($n > 1$, $h = 0$) is always unstable.

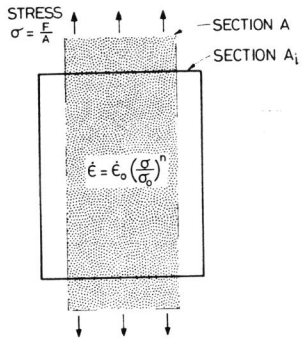

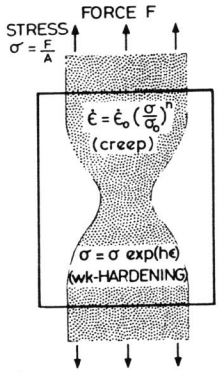

Fig. 11. Damage by loss of section.

Fig. 12. Necking in creep. Considerable strain is possible before a neck first forms.

Experiments do not support this last prediction. Power-law creeping solids do neck in tension, but they seldom do so at small strains; typically a creep strain of 0.1 to 0.5 is necessary to create a detectable neck in a cylindrical tensile sample. This is because, initially, the rate of amplification of the neck is very slow. An approximate analysis by Burke and Nix (1975) shows that the strain at which necking first influences the creep rate is considerable. Their numerical results for the strain ε_n at which necking commences, can be re-expressed as:

$$\varepsilon_n \simeq \frac{2}{n-1} \tag{4.7}$$

after a time t_n which we obtain from eqn. (4.3) as:

$$\dot{\varepsilon}_m t_n = \frac{1}{n}\{1 - \exp\frac{-2n}{n-1}\} \tag{4.8}$$

In thin sheet or wire, the onset of necking coincides, for practical purposes, with failure. Then eqns. (4.7) and (4.8) can be regarded as defining the failure strain ε_f and time t_f with the result that the creep damage tolerance λ is given by:

$$\lambda = \frac{2n}{1-n} \gtrsim 2$$

For other geometries the strain between the start of necking and final failure can be large; then $\lambda > 2$. If the sample is short and fat, considerable further extension is possible before final failure.

The treatment of necking is incomplete. To describe it properly we need equations (like eqn. 3.3) describing the rate at which the neck grows, and its effect on the creep rate. These must await further work.

Damage by Loss of Internal Section

Commonly, creep damage takes the form of voids or cracks, often on grain boundaries. A void or a crack can grow during creep by the diffusion of atoms away from it, or by the plastic flow of the material which surrounds it, or by a combination of both. In this section, we review ideas about void growth. The main points which emerge are these: that the damage and strain rates can be expressed in the form of eqns. (3.3); that when the damage is large ($w \gtrsim 1$) the results are identical to those assumed in the continuum treatment; but that when w is small, there are significant differences.

(a) Purely diffusional growth: boundary diffusion control. Hole growth controlled by boundary diffusion alone, is shown in Fig. 13. Matter diffuses out of the growing void and plates onto the grain boundary. If surface diffusion is rapid, matter distributes quickly within the void allowing its shape to remain near-spherical. The diffusion problem can be analysed with more than enough precision for our purposes (Hull and Rimmer, 1959; Speight and Harris, 1967; Raj and Ashby, 1975; Cocks and Ashby, 1982). The result is:

$$\frac{dw_2}{dt} = \dot{\varepsilon}_o \phi_o \left(\frac{\sigma}{\sigma_o}\right) \frac{1}{w^{\frac{1}{2}} \ell n\,(1/w_2)} \tag{4.9a}$$

$$\frac{d\varepsilon}{dt} = \dot{\varepsilon}_o \phi_o \left(\frac{\sigma}{\sigma_o}\right) \left\{\frac{2\ell}{d\,\ell n\,(1/w_2)}\right\} \tag{4.9b}$$

Here w_2 is the area fraction occupied by the void ($w_2 = r_h^2/\ell^2$); where ℓ is the spacing of the growing voids, d is the grain size, and ϕ_o is a temperature dependent material property which includes the relevant diffusion coefficients (Cocks and Ashby, 1982). The growth of the void increases the damage (eqn. 4.9a) and also gives strain (eqn. 4.9b). (At the same time, diffusional flow, or "Nabarro-Herring Coble" creep, may also contribute to the creep strain, but when the void spacing is less than the grain size, its contribution is small.)

When $w_1 = w_i$ (the initial damage level), we find the initial strain rate:

$$\dot{\varepsilon}_m = \dot{\varepsilon}_o \phi_o \left(\frac{\sigma}{\sigma_o}\right)\left(\frac{2\ell}{d\,\ell n\,(1/w_i)}\right) \tag{4.10}$$

allowing ϕ_o to be eliminated to give:

$$\boxed{\frac{dw_2}{dt} = \dot{\varepsilon}_m \left\{\frac{d}{2\ell\, w_2^{\frac{1}{2}}} \frac{\ell n\,(1/w_i)}{\ell n\,(1/w_2)}\right\}} \tag{4.11b}$$

$$\boxed{\frac{d\varepsilon}{dt} = \dot{\varepsilon}_m \left\{\frac{\ell n\,(1/w_i)}{\ell n\,(1/w_2)}\right\}} \tag{4.11b}$$

When w_2 is close to 1, the term $\ell n\,(1/w_2)$ reduces to $(1 - w_2)$, and these equations take on exactly the form proposed by Kachanov. But when w_2 is small, the damage rate is more complicated. In particular, the damage rate decreases as the damage grows; and it is generally when w_2 is small that diffusional growth is important.

The time to failure (and the Monkman-Grant constant) is obtained by integrating

Fig. 13. Damage by the diffusional growth of voids on grain boundaries. When boundary diffusion controls growth, the voids are roughly spherical.

Fig. 14. The growth of voids on grain boundaries controlled by surface diffusion. The voids are crack-like.

eqn. (4.11a):

$$C_m = \dot{\varepsilon}_m t_f \approx \tfrac{4}{3} \frac{\ell}{d} w_c^{\frac{1}{2}} \qquad (4.12)$$

where w_c is the critical damage at which some other mechanism, giving fast fracture, takes over. C_m falls as both the density of voids and the grain size increase. The strain ε_f, at constant stress, is given by simple geometry (Cocks and Ashby, 1982) by:

$$\varepsilon_f = \dot{\varepsilon}_m t_f + \tfrac{4}{3} w_c^{\frac{3}{2}} \frac{\ell}{d} \approx \tfrac{8}{3} \frac{\ell}{d} w_c^{\frac{1}{2}}$$

Then the creep-damage tolerance, λ, is given by

$$\lambda = \frac{\varepsilon_f}{\dot{\varepsilon}_m t_f} \approx 2$$

A more precise calculation gives $1.5 < \lambda < 2.5$ when this mechanism acts alone.

(b) Purely diffusional growth: surface diffusion control. Voids can remain near-spherical only if surface diffusion across the void surface is rapid. When it is not, matter flows out of the periphery of the void (by boundary diffusion) extending the void in the boundary plane as shown in Fig. 14. Then the damage-rate and the strain rate depend on both the rate of surface diffusion and on that of boundary diffusion (Chuang and Rice, 1973; Chuang et al., 1979; Cocks and Ashby, 1982). If, as before, we measure damage by the area-fraction of boundary occupied by the voids, we find (Cocks and Ashby, 1982):

$$\frac{dw_3}{dt} = \dot{\varepsilon}_o \psi_o w_3^{\frac{1}{2}} \left(\frac{\sigma}{\sigma_o (1 - w_3)}\right)^3 \qquad (4.13a)$$

$$\frac{d\varepsilon}{dt} = 4\dot{\varepsilon}_o \psi_o w_3^{\frac{1}{2}} \frac{\gamma}{d\sigma} \left(\frac{\sigma}{\sigma_o (1 - w_3)}\right)^3 \qquad (4.13b)$$

where γ is the surface energy of the material and ψ_o is a temperature dependent parameter containing the surface diffusion coefficient (Cocks and Ashby, 1982). As before, diffusional flow will contribute to the strain rate if the grain size is small enough, but we shall ignore it for the present. Normalising by the minimum creep rate $\dot{\varepsilon}_m$ (that for which $w_3 = w_i$) gives:

$$\frac{dw_3}{dt} = \dot{\varepsilon}_m \frac{d\sigma}{4\lambda} \left(\frac{w_3}{w_i}\right)^{\frac{1}{2}} \left(\frac{1 - w_i}{1 - w_3}\right)^3 \qquad (4.14a)$$

$$\frac{d\varepsilon}{dt} = \dot{\varepsilon}_m \left(\frac{w_3}{w_i}\right)^{\frac{1}{2}} \left(\frac{1 - w_i}{1 - w_3}\right)^3 \qquad (4.14b)$$

When w_3 is near unity, these become identical with eqns. (3.3) (as before); but when w_3 is small, the differences are significant. This result can be integrated to give the time to fracture and thus the Monkman-Grant constant for this mechanism acting alone:

$$C_m = \dot{\varepsilon}_m t_f = \frac{8\gamma}{d\sigma} (w_i w_c)^{\frac{1}{2}}$$

The strain to fracture at constant stress, ε_f, is just:

$$\varepsilon_f = \dot{\varepsilon}_m t_f$$

because the flat voids have negligible volume. Thus the Monkman-Grant "constant" decreases as the stress increases, and the creep-damage tolerance, λ, is close to unity. This is a particularly damaging mechanism giving crack-like damage and low ductility.

(c) Void growth by power-law creep. A void can grow by power-law creep of the surrounding matrix as shown in Fig. 15. Towards the end of life, when the damage is large, this mechanism always, ultimately, takes over. The void growth rate can be calculated by approximate methods (Edward and Ashby, 1979; Cocks and Ashby, 1982). In simple tension, the zone between the broken lines on Fig. 15 extends a little faster than the rest of the material, by a factor of $(1 / (1 - w_4))$, where $w_4 = r_h^2 / \ell^2$. But it is constrained by its surroundings so that it dilates, causing the hole to grow in volume, thereby increasing the damage w_4. This growth rate leads to a damage rate and strain rate (Cocks and Ashby, 1982) given by:

$$\frac{dw_4}{dt} = \dot{\varepsilon}_m \left\{\frac{1}{(1 - w_4)^n} - (1 - w_4)\right\} \qquad (4.16a)$$

$$\frac{d\varepsilon}{dt} = \dot{\varepsilon}_m \left\{1 + \frac{2r_h^o}{d} \left(\frac{1}{(1 - w_4)^n} - 1\right)\right\} \qquad (4.16b)$$

where $\dot{\varepsilon}_m$, as before, is the minimum creep rate (eqn. 3.2): and r_h^o is the initial radius of the voids. When w_4 approaches 1, these equations again reduce to the continuum result (eqns. 3.3) but when w_4 is small, they differ from eqns. (3.3) significantly.

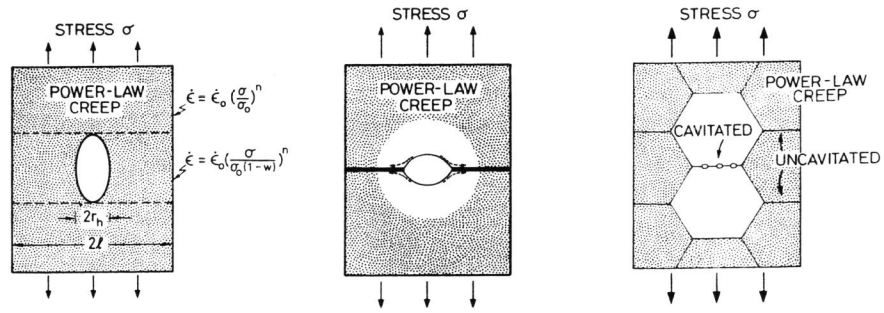

Fig. 15. The growth of voids by power-law creep alone; such voids have no special advantage if they lie on a grain boundary and are distributed throughout the creeping solid.

Fig. 16. The growth of voids by coupled diffusion and power-law creep:
(a) creep-enhanced diffusional growth;
(b) creep-constrained diffusional growth.

The time to failure is obtained by integrating eqn. (4.16a), giving, for constant stress:

$$C_m = \dot{\varepsilon}_m t_f = \frac{1}{(n+1)} \ln \left\{ \frac{1}{(n+1) w_i} \right\} \qquad (4.17)$$

and the strain to failure is simply:

$$\varepsilon_f = \dot{\varepsilon}_n t_f + \tfrac{4}{3} w_c^{\frac{1}{2}} \frac{\ell}{d} \qquad (4.18)$$

where w_i is the initial damage and w_c is the terminal damage. The creep damage tolerance is:

$$\lambda = 1 + \frac{\tfrac{4}{3} (n+1) w_c^{\frac{1}{2}} \ell/d}{\ln \left(\frac{1}{(n+1) w_i} \right)} \approx 1$$

at constant stress. When this mechanism acts alone, strains to fracture will be large. In tension, the life is then limited by other mechanisms - usually, loss of section and necking (Section 4.1). Materials with these characteristics include the important 304 and 316 stainless steels.

(d) Void growth by coupled diffusion and power-law creep ("creep-assisted" and "creep-constrained"). Experiments suggest that, frequently, voids grow by coupled mechanisms. Figure 16a shows one such case: matter flows out of the voids by diffusion, plating onto the boundary nearby. This causes a local wedging which, locally, unloads the boundary, removing the driving force for further diffusion. But if the material further away (shaded) undergoes power-law creep, then load is transferred back onto the region containing the void. Growth then depends on a coupling of diffusion and power-law creep, and is faster than by either mechanism acting alone. The problem has been analysed for various goemetries by Beere and Speight (1978); Needleman and Rice (1980); Cocks and Ashby (1980, 1982). The net result is that the void grows with a shape determined by local diffusion (and thus is either near-spherical, or crack-like) but with kinetics determined by the remote power-law creep (giving a time to fracture which depends on σ^n).

A second case is shown in Fig. 16b. If voids nucleate on some grain facets but not on others, then a pair of grains which have voids on a shared boundary may be surrounded by a shell of grains which are undamaged. The problem has been analysed by Dyson (1976, 1979) who calls it "constrained cavity growth" because, if the voids are to grow, the surrounding shell of grains must deform also, and this requirement may restrict the growth: this time the growth is slower than that by diffusion alone. But, as before, the voids grow with a shape which is determined by local diffusion but with kinetics determined by the remote power-law creep.

Both of these coupled mechanisms can be analysed; the results can be found in the references cited already. For the present purposes we note that the values of C_m, ε_f and λ which characterise them are intermediate between those of the separate contributing mechanisms.

(e) Loss of section by growth of a single dominant crack. When the creep-damage tolerance of the material is low, damage may coalesce to form a single, dominant crack. A zone of more intense damage forms at its tip (within which any of the previous mechanisms may operate) and the crack grows into this zone (Fig. 17). The damage is now localised, and the response of the sample can no longer be described by continuous damage mechanics; instead, a time-dependent J-integral approach must be used (see, for example, Wilkinson and Vitek, 1982). This is a separate topic which we will not pursue here.

Damage by Degradation of Microstructure

Tertiary creep is not always associated with loss of section. Engineering alloys which are particularly designed to resist deformation often enter tertiary creep without any sign of cavitation or cracking; cavity damage appears only when tertiary creep is well established. The damage in this case is a kind of time or strain-induced softening of the material, and is associated with changes in its microstructure. This can arise in two ways: by the thermal coarsening or dissolution of precipitate particles (Fig. 18) and by the formation of a creep substructure which permits an acceleration of the creep rate (Fig. 19 and 20): it is really a sort of primary creep, though the shape of the creep curve is like that of a conventional tertiary. From an engineering standpoint, these mechanisms can be insidious since there are no cracks or voids to indicate that damage has accumulated.

(a) Thermal coarsening of particles. Most engineering alloys for use at high temperatures derive an important part of their creep strength from a fine dispersion of particles: carbides in ferritic creep-resistant steels, and γ' in the superalloys, are examples. At service temperatures, these slowly coarsen and the coarsening causes a gradual loss of strength and an acceleration of creep (Figs. 6 and 18). It has been suggested that this could be the origin of tertiary creep in these alloys (Williams and Cane, 1979; Burt et al., 1979; Tipler and Peck, 1981; Stevens and Flewitt, 1979). We approach the problem by combining an equation for the creep of dispersion hardened alloys with one describing the coarsening of the dispersion (Dyson and McLean, 1983).

There is an increasing body of experimental evidence (Haasen et al., 1984) that, from the early stages of decomposition onwards, the volume fraction of particles in precipitation-hardened alloys is almost constant. The particles coarsen with time, following the diffusion-controlled coarsening law of Wagner (1961) and Lifshitz and Slyozov (1961):

$$\frac{dr}{dt} = \frac{K}{3r^2} \qquad (4.21)$$

so that the particle diameter after time t is given by:

$$r^3 = r_o^3 + Kt \qquad (4.22)$$

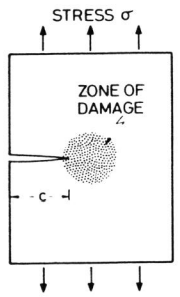

Fig. 17. The growth of a single, dominant crack.

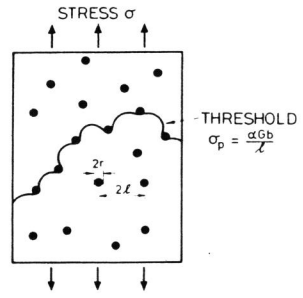

Fig. 18. Damage by particle coarsening or dissolution. Either process increases the obstacle spacing (ℓ) and lowers the threshold stress σ_p.

Here K is a constant which includes the diffusion coefficient for transport of the material of which the particle is made, and r is the initial particle size. The spacing of the particles relates to their size through the volume fraction so that ℓ increases with time as: .

$$\ell^3 = \ell_o^3 (1 + K't) \tag{4.23}$$

where ℓ_o is the initial spacing and K' is another kinetic constant. It might be thought that creep would accelerate coarsening, but Gibbons and Hopkins (1972), Martin and Doherty (1976) and Sauthoff (1983), who studied the effect of creep flow on the coarsening of particles in a number of alloys, found the acceleration to be negligible. Then we may use the simple Wagner/Lifshitz law (4.22) to model particle coarsening during creep.

To do so, we require a modified creep equation which includes the effect of the particles on the creep rate. The fundamentals of this problem have been examined by Shewfelt and Brown (1974, 1977),Gibeling and Nix (1980) Arzt and Ashby (1983), Petersein and Sauthoff (1983) and others. There is considerable evidence that the creep rate of particle-containing alloys is well described by a modified form of Norton's Law (Threadgill and Wilshire, 1974; Davies et al., 1973; Parker and Wilshire, 1975; Evans and Harrison, 1976):

$$\dot{\varepsilon} = \dot{\varepsilon}_o \left(\frac{\sigma - \sigma_p}{\sigma_o}\right)^n \tag{4.24}$$

where the threshold stress, σ_p, is close to the Orowan stress (Fig. 18):

$$\sigma_p \approx \alpha \frac{Gb}{\ell} \tag{4.25}$$

Here G is the shear modulus, b the Burgers vector and α a constant, near unity. Assembling these results gives the time-dependent creep law:

$$\dot{\varepsilon} = \dot{\varepsilon}_o \left(\frac{\sigma}{\sigma_o}\right)^n \left\{1 - \frac{\sigma_p^o \sigma}{(1 + K' t)^{\frac{1}{3}}}\right\}^n \tag{4.26}$$

where $\sigma_p^o = \alpha Gb/\ell_o$.

We now define damage w_s as a state variable, with the range 0 to 1 (as usual) such that:

$$w_s = 1 - \frac{1}{(1 + K' t)^{\frac{1}{3}}} \tag{4.27}$$

Then:

$$\frac{dw_s}{dt} = (1 - w_s)^4 \frac{K'}{3} \tag{4.28a}$$

$$\frac{d\varepsilon}{dt} = \dot{\varepsilon}_o \left(\frac{\sigma}{\sigma_o}\right)^n \{1 - (\sigma_p^o/\sigma)(1 - w_s)\}^n \tag{4.28b}$$

from which the time to fracture is:

$$t_f = \left\{\frac{1}{(1 - w_c)^3} - 1\right\} / K' \tag{4.29}$$

and the strain ε_f is approximately (for $\sigma >> \sigma_p^o$):

$$\varepsilon_f = \dot{\varepsilon}_o \left(\frac{\sigma}{\sigma_o}\right)^n \frac{1}{(1 - w_c)^3} K' \tag{4.30}$$

In this instance the minimum creep rate is, of course,

$$\dot{\varepsilon}_m = \dot{\varepsilon}_o \left(\frac{\sigma - \sigma_p^o}{\sigma_o}\right)^n$$

so that

$$\lambda = \frac{\varepsilon_f}{\dot{\varepsilon}_m t_f} = \frac{1}{(1 - \sigma_p^o/\sigma)^n}$$

Now, if the stress is near the initial value of the threshold stress σ_p^o (as it will be in any long-term test) the creep-damage tolerance is very large: 10 or more.

These equations describe the effect of simultaneous ageing on creep. The effect is most marked at low stress levels (because the factor σ_p^o/σ is then large). Changes in the initial particle dispersion (determining σ_p^o) have an important effect on creep rate, and σ_p is independent of σ. These qualitative ideas are supporated by the observations of Stevens and Flewitt (1979), who tested the cast superalloy IN738LC, and of Petersein and Sauthoff (1983) and Cane and Silcox (1982) who studied ferritic steels containing carbides.

But this not the whole story. Dyson and McLean (1983), in a careful analysis of data for nickel-based superalloys, conclude that tertiary creep is not solely a consequence of the coarsening of the γ' particles but is due primarily to another, quite different, way in which structural changes cause creep rates to accelerate with time. The underlying ideas are that strain can increase the mobile dislocation density, and that it can also enhance the rate of local recovery. We term it "substructure-induced tertiary creep".

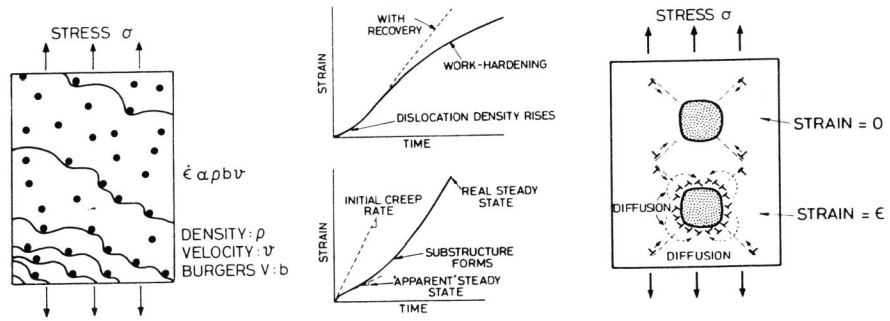

Fig. 19. Accelerating creep caused by increase in mobile dislocation density.

Fig. 20. Creep curves produced by increase in mobile dislocation density (above) or the formation of a substructure (below). The curves are obtained by integratring equations given in the text, with appropriate values of the constant and coefficients.

Fig. 21. Accelerating creep caused by formation of a creep-enhancing substructure.

(b) Substructure-induced acceleration of creep. During the creep of pure metals and solid solutions, dislocations move (giving creep strain) and they accumulate (causing hardening). The creep rate is rapid at first, and then slows down. As the density of dislocations increases, recovery mechanisms (climb, cross slip, diffusional accommodation at cell walls, etc.) allow annihilation, and the removal of long-range stress; as hardening and recovery rates come into balance, the creep rate approaches a steady-state value. The overall result is a "normal" transient, concave downwards.

There are two ways in which a different, concave-upwards, transient can occur; and this anomalous transient appears, on a creep curve, as a pseudo-tertiary like those observed in superalloys. The first relates to the density of mobile dislocations (Dyson and McLean, 1983). When a density ρ of dislocation with Burger's vector b moves at velocity v, the strain rate (Fig. 19) is given by:

$$\dot{\varepsilon} = \rho b v \qquad (4.30)$$

The velocity v depends on the effective stress σ_{eff}:

$$\sigma_{eff} = \sigma - \alpha G b \sqrt{\rho} \qquad (4.31)$$

where the second term is the internal stress due to the other dislocations. As strain accumulates, ρ increases; Alexander and Haasen (1968) show that:

$$\frac{d\rho}{dt} = \frac{\rho v}{L} \qquad (4.32)$$

where L is a characteristic slip-distance for multiplication. The behaviour depends on L and the relation between v and σ_{eff}. When (Fig. 19) dislocations move through a field of particles at stresses well below that required for Orowan bowing ($\sigma_p = \alpha Gb/\ell$), as in superalloys, their motion must be climb-limited. Then the velocity v depends, on a low power of σ_{eff}. When equations (4.30) and (4.32) are integrated as a coupled set, with $v = B\,\sigma_{eff}$, they give a creep curve with an inverse transient, caused by dislocation-mobility limited creep as shown in Fig. 20(a) (Alexander and Haasen, 1969). The extent with a length that depends on the parameter L. The formulation neglects recovery; if that is included, the transient leads into steady-state flow. The "damage", in this case, is related to the mobile dislocation density.

At low streses ($\sigma \approx 0.1\ \sigma_y$), this offers an explanation for the dislocation-structure induced tertiary. But the observations of Henderson and McLean (1983) at higher stresses ($\sigma \approx 0.5\ \sigma_y$) suggest a second possible explanation. Micrographs of superalloys deformed in creep (Fig. 7) show the development of a well-defined network of dislocations encasing each γ' particle. It appears that, on loading in the creep regime, dislocations move but cannot penetrate the particles, so they loop around them. The back stress from these loops is large and the creep rate falls. As straining proceeds, a network of dislocations (like a cell wall) forms around each particle (Fig. 21). This network, like the cells in pure metals allows diffusion from one part of the cell wall to another, relieving the back-stress; once formed, the cellular network provides a recovery mechanism.

It is possible to illustrate this more formally. Let the creep rate be given by:

$$\frac{d\varepsilon}{dt} = \dot{\varepsilon}_0 \left(\frac{\sigma - \sigma_i}{\sigma_o}\right)^n \qquad (4.33)$$

where σ_i is an internal stress, caused by the back-stress from the non-deforming particles. It increases with strain, but it is diminished by recovery:

$$d\sigma_i = H d\varepsilon - R\varepsilon\,\sigma_i\,dt \qquad (4.34)$$

Here H is a hardening coefficient (with dimensions of stress), and R a kinetic constant (with dimensions of s^{-1}). The first term describes the hardening, and is independent of strain; the second describes the recovery and increases the strain. The recovery rate depends on the internal stress (because it is σ_i which drives recovery) and the strain ε (because the density of the network increases linearly with strain). When this pair of differential equations is integrated numerically they give a creep curve which shows an inflection from which the creep rate accelerates as the network forms, giving a pseudo-tertiary (Fig. 20b). In fact, the true steady state has not been reached - it is approached at the end of the creep curve. The "damage" is the network.

The reader may question the assumptions underlying the development of these models for dislocation-substructure induced tertiaries. The important point is simply that the creep rate depends on the mobile density of dislocations, and on the recovery rate. Both evolve with strain and may lead to an acceleration of the creep rate. The result is not a true tertiary; in the absence of other damage mechanisms, they lead to a new steady state, not to fracture. But the large increase in creep rate they produce may, in practice, constitute failure. Both mechanisms accelerate creep (reducing t_f) but do not alter ε_f (which is determined by other mechanisms) so the value of λ is large, typically greater than 5.

Damage by Gas-Environmental Attack

Exposure to air or to other aggressive gasses during creep generally changes the rupture life and ductility. At low stresses and temperatures the creep rate is often lower, and the life is longer, in air than it is in vacuum (because the oxide has a higher creep strength). But at higher stresses or temperatures, environmental attack accelerates creep and reduces life. The low-alloy ferritic steels, for example, form oxides which spall, reducing the load-bearing section and accelerating creep (Cane and Manning,1981). Nickel and its alloys (including the superalloys) can suffer in a different way: exposure to oxidising atmospheres before, or during, creep can increase the creep rate dramatically and reduce both the creep life and the ductility (Tien et al., 1976; Woodford et al., 1982; Pandey et al., 1984). It has been suggested that this loss of life might be caused by void growth, enhanced by extra vacancies injected at the metal/oxide interface as a by-product of the way in which the oxide grows (Hancock and Fletcher, 1966; Caplan et al., 1980); or that the loss of life might be due to internal stresses caused by the volume change when surface oxide forms (Harris, 1978). Neither explanation is consistent with the bulk of the experimental data (Bricknell and Woodford, 1982; Pandey et al., 1984), which point to internal oxidation as the cause of the enhanced cavitation. We now examine these two mechanisms in more detail, starting with internal oxidation.

(a) Damage by internal oxidation. On heating in an oxidising atmosphere, oxygen penetrates the component unless it forms a protective surface oxide which remains intact even under creep. The inward diffusing oxygen reacts with impurities to give a precipitate of an oxide: solid if the impurity is metallic, gaseous if the impurity is either carbon or hydrogen. For kinetic reasons, second phases of all kinds will usually nucleate more

frequently and grow more quickly on grain boundaries to give an array of bubbles or particles as shown in Fig. 8. Both act as nuclei for further void growth, and degrade the strength (Woodford, 1981; Bricknell et al., 1982; Bricknell and Woodford, 1982a,b; Pandey et al., 1984).

This damage mechanism can be modelled and expressed in the standard form we have used for the others. Consider the simplest case: a cylindrical sample is loaded in tension, at elevated temperatures and in an oxidising atmosphere (the extension to the other geometries will be obvious). Oxygen diffuses inwards, reacting with the most readily oxidised impurities, which precipitate as oxides (Fig. 22). The depth x of this internally oxidised layer (Rhines, 1940; Meijering and Druyvesteyn, 1947) increases with time (for $x/R >> 1$) as:

$$\frac{dx}{dt} = \frac{K}{2x} \qquad (4.35)$$

where K is a kinetic factor which includes the diffusion coefficients of oxygen and of the impurities. The depth x then increases parabolically with time:

$$x^2 = Kt$$

If this zone of internal oxidation carries no load, then the damage w_7 can be defined as the area-fraction of the cross-section in which internal oxidation has taken place:

$$w_7 = \frac{2x}{R}\left(1 - \frac{x}{2R}\right) \approx \frac{2x}{R} \qquad (4.36)$$

The load is carried by the remaining section, which occupies a fraction $(1 - w_7)$ of the section. Thus:

$$\frac{dw_7}{dt} = 2K/w_7\, R^2 \qquad (4.37a)$$

$$\frac{d\varepsilon}{dt} = \dot{\varepsilon}_o \left(\frac{\sigma}{\sigma_o (1 - w_7)}\right)^n \qquad (4.37b)$$

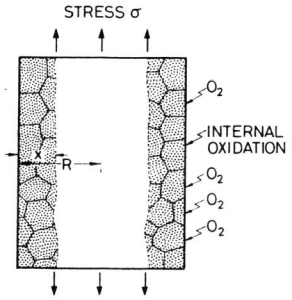

Fig. 22. Damage by internal oxidation (or other, similar, penetration by a reactive gas).

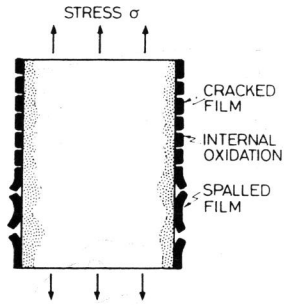

Fig. 23. Damage by external oxidation (or attack by other aggressive gases).

The equations show that environmental attack can be expressed in the same format as the other damage mechanisms. The difference is that the damage is no longer a state variable, but (because the damage propagates inward from the surface) depends on the dimensions R of the sample. Integrating the first of these equations gives the time to failure when the mechanism operates alone:

$$t_f = \frac{R^2 w_c^2}{4K}$$

It depends on sample size (for obvious reasons); doubling the sample dimensions increases the life by a factor of 4. The strain to failure is obtained by integrating eqn. (4.37b):

$$\varepsilon_f = \frac{\dot{\varepsilon}_m R^2}{2K}\left\{\frac{1}{n-1}\left(\frac{1}{(1 - w_c)^{n-1}} - 1\right) - \frac{1}{n-2}\left(\frac{1}{(1 - w_c)^{n-2}} - 1\right)\right\}$$

The creep-damage tolerance λ is independent of R. It is unity when w_c is small, but rises towards infinity as w_c approaches 1.

(b) Damage by failure of a protective oxide film. Some pure metals (such as aluminium) form protective oxides, and many alloys contain components (such as chromium) which oxidise preferentially to give a protective surface film. During creep, the oxide film is stretched, and may fail (Manning, 1981; Riedel, 1982) as shown in Fig. 23. If it does, environmental attack restarts at the cracks. Other, less protective oxides, may still impede the access of oxygen to the metal surface, and again it is the cracking or spalling of the oxide which permits further attack (Fig. 9). In both cases, the rate of attack is no longer controlled by the inward diffusion of oxygen, but by the frequency of surface cracking; and instead of depending only on time (as simple oxidation does) it depends also on the strain-rate.

Oxides generally creep more slowly than the metal from which they form. If the section of the test piece is small then the oxide suppresses creep and extends life. In engineering components, it is more usual that the section size is large compared to the oxide thickness. Then creep of the metal loads the film, which fractures or spalls and carries little or no load. The details, of course, depend on the alloy and the environment; but it is instructive to examine how the mechanism might be modelled, and the form of the resulting equations.

Consider a brittle, external oxide, of thickness h, on the surface of a creeping metal. The fracture strain (or spalling strain) of the oxide is ε^*. Creep of the underlying metal stretches the film until it fractures or spalls, as shown in Fig. 23. This increases the oxidation rate locally until the crack or gap heals again; the time constant for healing is t^*. The time taken for the new oxide film to crack is:

$$t^* = \frac{\varepsilon^*}{\dot{\varepsilon}}$$

During this time, the film has grown (assuming parabolic kinetics) to a thickness:

$$x^* = \sqrt{2K_p t^*}$$

where K_p is the parabolic rate constant (units: m^2/s). If the oxide spalls when it fractures, the rate of loss of thickness of the sample, dX/dt, is:

$$\frac{dX}{dt} \simeq \frac{X^*}{t^*} \simeq \left(\frac{2K_p \dot{\varepsilon}}{\varepsilon^*}\right)^{1/2} \qquad (4.38)$$

or, defining damage as the fractional loss of section, for a cylindrical sample of radius R,

$$\frac{dw_s}{dt} = \frac{2}{R}\left(\frac{2K_p\,\dot{\varepsilon}}{\varepsilon^*}\right)^{1/2} \qquad (4.39a)$$

$$\frac{d\varepsilon}{dt} = \dot{\varepsilon}_o\left(\frac{\sigma}{\sigma_o\,(1 - w)}\right)^n \qquad (4.39b)$$

Note that the loss of section is linear in time (at constant ε), even though the kinetics of oxidation are parabolic. For samples of a constant initial size, R, these equations have the form of the Kachanov equations (3.3), with $m = n/2$. Integrating the first gives the time to failure for this mechanism acting alone:

$$t_f = \frac{R}{n+2}\left(\frac{\varepsilon^*}{2K_p\,\dot{\varepsilon}_m}\right)^{1/2}\{1 - (1 - w_c)^{n/2}\}$$

The time to failure now depends on the sample radius (for obvious reasons). The strain to failure:

$$\varepsilon_f = \frac{R}{(n-2)}\left(\frac{\dot{\varepsilon}_m\,\varepsilon^*}{2K_p}\right)\left\{\frac{1}{(1 - w_c)^{\frac{n}{2}} - 1} - 1\right\}$$

from which:

$$\lambda = \frac{n+2}{n-1}\,\frac{\frac{1}{(1 - w_c)^{\frac{n}{2}}} - 1^{-1}}{1 - (1 - w_c)^{n/2}}$$

Note that λ is independent of R. It has the limit $(n + 2)/n \to 1$ when w_c is small, but increases towards infinity as w_c approaches 1.

DISCUSSION AND CONCLUSIONS

There are many mechanisms of tertiary creep; some eight have been analysed here, and there are certainly others. Each can be thought of as introducing its own kinds of "damage" into the material which accelerates creep and contributes to the tertiary. Ultimately, one component of damage reaches a fatal level and the sample fails. Damage mechanisms may interact: void-damage may grow at first by diffusion, but later by power-law creep, for example; or substructure-damage may cause the tertiary, but be interrupted by void-damage or by necking to give a final failure.

We have considered the mechanisms in isolation, and have not yet attempted the difficult problem of their superposition. With this simplification, we find that each mechanism can be described by a pair of coupled differential equations, one describing the rate at which damage accumulates, the other describing the strain rate. When this is done, a close parallel emerges between the materials scientist's view of creep damage and that which forms the basis of the continuum theory of creep of Kachanov, Rabotnov, Hult and Leckie, summarised in Section 2. In all cases, the response of the material is described by a pair of differential equations:

$$\frac{dw}{dt} = f(\sigma, T, w) \qquad (5.1a)$$

$$\frac{d\varepsilon}{dt} = g(\sigma, T, w) \qquad (5.1b)$$

where f and g are functions, explicitly given in the text; for many mechanisms f and g are well approximated by the functions (3.3) assumed by Kachanov and others. The time to failure t_f is obtained by integrating the first; the strain to failure ε_f and the creep damage tolerance, λ, by integrating the second. The shape of the creep curve and the behaviour under varying stress and temperature, are obtained by integrating the pair simultaneously.

The great strength of the continuum, approach is its generality. The difficulty is that there is not one, but eight or more mechanisms which can potentially contribute to damage. Some are associated with large values of λ and ε_f, and are not intrinsically as dangerous as those with low values of λ and ε_f. Under the restricted conditions of most engineering applications, it is likely that fewer - perhaps only one or two - mechanisms contribute in an important way to tertiary creep and failure; that may be why the continuum method has been found useful in engineering practice. But the dangers of assuming that a single mechanism is always dominant are obvious: a change of conditions which cause a change in mechanism will give lives which are less - sometimes much less - than those predicted.

So it is interesting, from both a scientific and an engineering point of view, to have some idea of the dominant mechanism of creep damage. One way of identifying a mechanism is by careful microscopy; but in an engineering environment, this may be impractical. We have found that some information about mechanisms can be obtained simply from the shape and scale of the creep curve. The information is contained in the quantities C_m, ε_f and λ, all of which can be read from a single creep curve for the material under service conditions. Figure 24(a) shows a diagnostic figure, constructed from the information given earlier in the text. The axes are ε_f and C_m ($= \dot{\varepsilon}_m\,t_f$). The areas show the regimes associated with each class of mechanism. As an example: when creep occurs at <u>constant stress</u>, void growth mechanisms all lie within the area delineated by $\lambda = 1$ and $\lambda = 2.5$ (Section 4.2). Under the more usual condition of <u>constant load</u>, the extent of this region is reduced because damage by loss of external section occurs at the same time; the dotted region illustrates this for a material with a stress exponent $n = 3$. The dashed line $n = 5$, shows the effect of n in truncating the void growth regime. The chain line denotes the onset of necking at values of n between 5 and 10 (eqn. 4.7) and thus separates the regimes where life is terminated by low λ mechanisms from those in which necking may intervene. If data from a test are plotted onto the figure, then an idea of the dominant mechanism (the one primarily responsible for tertiary and failure) can be obtained.
Figure 24(b) shows data for pure iron, a steel and a number of superalloys. In each case the prediction of the diagram agrees well with the observed mechanism of failure.

We believe that this information can be used to select the appropriate constitutive law (a pair of differential equations like eqns. (3.3) for engineering design against creep. The basic continuum approach outlined in Section 3, is, we have seen, too simple. Each mechanism can be described by a pair of such equations, but the detailed form of the equations depends on the mechanism, and it is this which determines the shape and scale (and thus C_m, ε_f and λ) of the creep curve. It may be that, empirically, the Kachanov equations (3.3) are flexible enough to describe all shapes of creep curve; but the effect of change of stress, or of specimen size, or of microstructure (like grain size) which is explicit in the model-based equations, is absent in the continuum approach. The next step, we believe, is to formulate simple modifications to eqns. (3.3) which incorporate, as far as possible, the general features of the microscopic models, but which avoid their complexity.

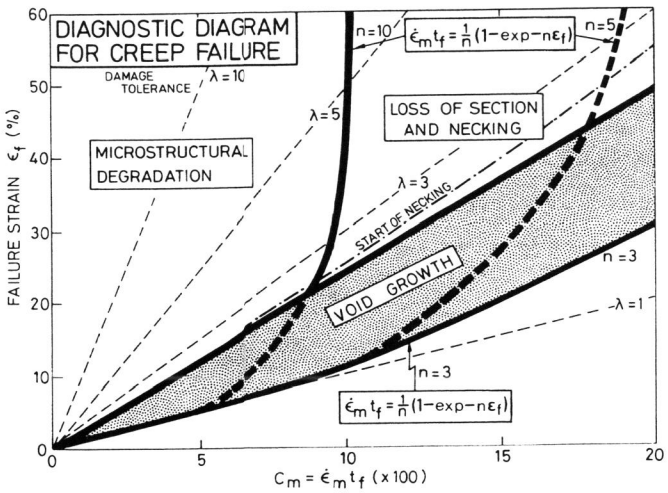

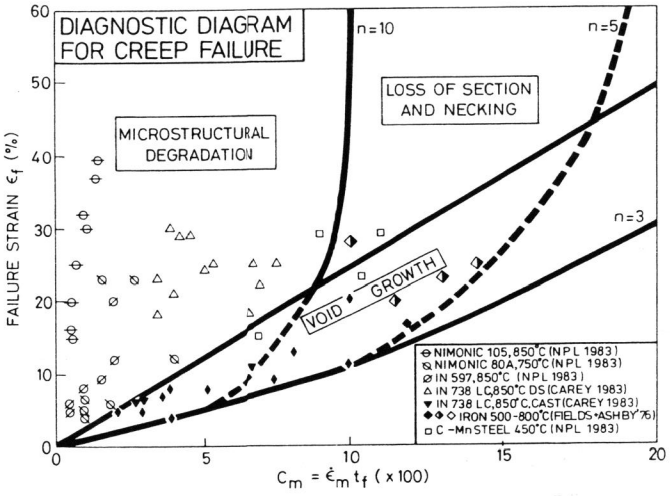

Fig. 24. A diagnostic diagram, showing the combinations of ϵ_f and C_m which characterise various mechanisms. The diagram gives information about mechanism (and thus choice of constitutive law) from data derived from the creep curve alone.

The identification of mechanism, and the possibility of a change of mechanism, is of particular importance in applying the life-fraction "Robinsons" rule (1952). If a single mechanism is dominant, and if the damage rate it causes can be expressed in a form in which the variables σ and D are separated:

$$\frac{dw}{dt} = f(\sigma)\, g(T)\, h(w) \qquad (5.2)$$

then the creep curve has a fixed shape (only its scale is changed by altering the stress or the temperature), and the life fraction rule:

$$\sum_i \frac{t_i}{t_{fi}} = 1 \qquad (5.3)$$

applies (Hult, 1974; Cocks and Ashby, 1982). Many of the mechanisms can be expressed in the form of eqn. (5.2), and for these, design based on eqn. (5.3) is valid. But anything that changes the shape of the creep curve - such as the appearance of a new mechanism - invalidates both eqns. (5.1) and (5.3). The shape of the creep curve is an indicator of mechanism; and of the validity of simplifying laws like Robinson's rule.

Much further work is needed to complete the unification of the continuum and the micromechanistic approaches to creep fracture. This paper has explored routes by which it might be achieved, and demonstrated, we hope, that the task is possible.

Acknowledgements

We acknowledge with gratitude a series of helpful discussions with Prof. F.A. Leckie. We are grateful for comments by Dr. M. McLean and Dr. P.J. Henderson.

REFERENCES

Alexander, H. and Haasen, P. (1968). Solid State Physics, 22, 27.
Arzt, E. and Ashby, M.F. (1983). Scripta Met., 16, 1285.
Barer, R.D. and Peters, B.F. (1970). Why Metals Fail, Gordon and Breach, p75.
Beere, W. and Speight, M.V. (1978). Met. Sci., 12, 172.
Burke, M.A. and Nix, W.D. (1975). Acta Met., 23, 793.
Bricknell, R.H., Mulford, R.A. and Woodford, D.A. (1982). Met. Trans., 13A, 1223.
Bricknell, R.H. and Woodford, D.A. (1982). Acta Met., 30, 257.
Bricknell, R.H. and Woodford, D.A. (1982). Scripta Met., 16, 761.
Burt, H., Dennison, J.P. and Wilshire, B. (1979). Metal. Sci., 13, 295.
Cane, B.J. and Manning, M.I. (1981). CERL Memorandum LM/MATS/407, CERL, Leatherhead, Surrey, U.K.
Cane, B.J. and Silcox, J. (1982). Private communication.
Carey, J.A. (1983). Ph.D. Thesis, Engineering Department, Cambridge University.
Caplan, D., Hussey, R.J., Sproule, G.I. and Graham, M.J. (1980). Oxid. Metals, 4, 279.
Chuang, T-J., and Rice, J.R. (1973). Acta Met., 21, 1625.
Chuang, T-J., Kagawa, K.I., Rice, J.R. and Sills, L.B. (1979). Acta Met., 27, 265.
Cocks, A.C.F. and Ashby, M.F. (1980). Metal Sci., 14, 395.
Cocks, A.C.F. and Ashby, M.F. (1982). Prog. Mat. Sci., p.1.
Cocks, A.C.F. and Ashby, M.F. (1982). Metal Sci., 16, 465.

Considere, A. (1885). Ann. Ponts. Chaussees, 9, 574.
Davies, P.W., Nelmes, G., Williams, K.R.W. and Wilshire, B. (1973). Metal Sci., 7, 87.
Dyson, B.F. and McLean, M. (1983). Acta Met., 31, 17.
Dyson, B.F. (1976). Metal Sci., 10, 349.
Dyson, B.F. (1979). Canad. Met. Quarterly, 18, 31.
Edward, G.H. and Ashby, M.F. (1979). Acta Met., 27, 1505.
Evans, W.J. and Harrison, G.F. (1976). Metal Sci., 10, 307.
Gilman, J.J. (1969). Micromechanisms of Flow in Solids, McGraw-Hill, Ch. 7.
Gibbons, T.B. and Hopkins, B.E. (1971). Metal Sci. J., 5, 233.
Haasen, P., Gerold, V. and Ashby, M.F., Eds., (1984). Acta/Scripta Conf. on The Early Stages of Decomposition of Alloys, Pergamon Press.
Hancock, P. and Fletcher, R. (1966). Metallurgie XI, 1.
Harris, J.E. (1978). Acta Met., 26, 1033.
Hart, E.W. (1967). Acta Met., 15, 351.
Henderson, P.J. and McLean, M. (1983) Acta Met. 31, 1203.
Henderson, P.J. (1984). NPL Report DMA (A) 72.
Hoff, N.J. (1953). J. Appl. Mech., 20, 1055.
Hull, D, and Rimmer, D.E. (1959). Phil. Mag., 4, 673.
Hult, J. (1974). In On Topics in Applied Continuum Mechanics. J.L. Zeman and F. Ziegler (Eds.), Springer, p137.
Kachanov, L.M. (1958). Izv. Akad. Nauk. SSSR, No. 8, p26.
Leckie, F.A. and Hayhurst, D.R. (1977). Acta Met., 25, 1059.
Lifshitz, I.M. and Slyozov, I. (1961). J. Phys. Chem. Solids, 19, 35.
Manning, M.I. (1981). Corrosion and Mechanical Stress at High Temperature, V. Guttmann and M. Merz (Eds.), Applied Science, Lond., p.323.
Martin, J.W. and Doherty, R.D. (1976). Stability of Microstructure in Metallic Systems, Cambridge University Press.
Meijering, J.L. and Druyvesteyn, M.J. (1947). Philips Research Report 2, No. 21, p.260.
Monkman, F.C. and Grant, N.J. (1956). Proc. Am. Soc. Testing Metals, 56, 593.
man, A. and Rice, J.R. (1980). Acta Met., 28, 1315.
Nibkin, K.M., Webster, G.A. and Turner, C.E. (1976). ASTM STP 601, 47.
Pandey, M.C., Dyson, B.F. and Taplin, D.M.R. (1984) Proc. Roy. Soc. 393, 117.
Parker, J.D. and Wilshire, B. (1975). Metal. Sci., 9, 248.
Petersein, J. and Sauthoff, G. (1983). In Deformation in Multiphase and Particle Containing Materials. J.B. Bilde Sorensen (Eds.), Riso National Labs., p.479.
Rabotnov, Yu N. (1969). Proc. XII IUTAM Congress, Stanford, Eds. Hetenyi and W.G. Vincenti, Springer, p.342.
Raj, R. and Ashby, M.F. (1975). Acta Met., 23, 653.
Riedel, H. (1982). Metal Science, 16, 569.
Rhines, F.N. (1940). Trans. AIME, 137, 246.
Robinson, E.L. (1952). Trans. Am. Inst. Min. Engrs., 7A, 777.
Sauthoff, G. (1983). Arch. Eisenhuttenweg 54, 151, 155 and 337.
Shewfelt, R.S.W. and Brown, L.M. (1974). Phil. Mag., 30, 1135; (1977) Phil. Mag., 35, 945.
Speight, M.V. and Harris, J.E. (1967). Metal Sci., 1, 83.
Stevens, R.A. and Flewitt, P.E.J. (1979). Mater. Sci. Engng., 37, 237.
Threadgill, P.L. and Wilshire, B. (1974). Proc. Conf. on Creep Strength of Steels, p8, Metals Soc., Lond.
Tien, J.K., Malu, M. and Purashothman, S. (1976). Alloy and Microstructural Design, Ch. 4, J.K. Tien and G.S. Ansell (Eds.). Acad. Press. N.Y.
Tipler, H.R. and Peck, M.S. (1981). NPL Report DMA (A) 33.
Wagner, C. (1961). Z. Electrochem., 65, 581.
Wilkinson, D.S. and Vitek, V. (1982). Acta Met. 30, 1723.
Williams, K.R. and Cane, B.J. (1979). Mat. Sci. and Eng., 38, 199.
Woodford, D.A. (1981). Met. Trans., 12A, 299.